Fibonacci numerical integration on a sphere

2004 J. Phys. A: Math. Gen. 37 11591

(http://iopscience.iop.org/0305-4470/37/48/005)

INSTITUTE OF PHYSICS PUBLISHING JOURNAL OF PHYSICS A: MATHEMATICAL AND GENERAL

J. Phys. A: Math. Gen. **37** (2004) 11591–11601 PII: S0305-4470(04)77257-1

Fibonacci numerical integration on a sphere

J H Hannay and J F Nye

H. H. Wills Physics Laboratory Tyndall Avenue, University of Bristol, Bristol BS8 1TL, UK

Received 5 March 2004, in final form 27 August 2004
Published 17 November 2004
Online at stacks.iop.org/JPhysA/37/11591
doi:10.1088/0305-4470/37/48/005

Abstract

For elementary numerical integration on a sphere, there is a distinct advantage in using an oblique array of integration sampling points based on a chosen pair of successive Fibonacci numbers. The pattern has a familiar appearance of intersecting spirals, avoiding the local anisotropy of a conventional latitude–longitude array. Besides the oblique Fibonacci array, the prescription we give is also based on a non-uniform scaling used for one-dimensional numerical integration, and indeed achieves the same order of accuracy as for one dimension: error $\sim N^{-6}$ for N points. This benefit of Fibonacci is not shared by domains of integration with boundaries (e.g., a square, for which it was originally proposed); with non-uniform scaling the error goes as N^{-3}, with or without Fibonacci. For experimental measurements over a sphere our prescription is realized by a non-uniform Fibonacci array of weighted sampling points.

PACS number: 02.30.Lt

1. General consideration

When integration over a surface has to be performed numerically a suitable distribution of sampling points must be chosen. The problem may arise in theoretical work when a specified continuous function is being integrated or in experimental work when an array of measured values is being used. An example of the latter would be measuring a microwave field over a sphere surrounding an antenna [1].

If a domain of integration has boundaries they are usually the main cause of numerical error (because of the discontinuities they imply). These are quantified, for example, in the Euler–Maclaurin summation formula [2] for a one-dimensional integral. If there are no boundaries, then, one can hope to find reduced error. For instance, in integration around a circle, simple equispaced integration points are optimal and give accuracy $\sim\exp(-\text{constant} \times N)$ for N points and an analytic integrand [3]. In two dimensions the same would apply to a torus, but a sphere is more difficult. It has no boundary, but there is no way of placing more than 60 integration points so that each has identical surroundings [4].

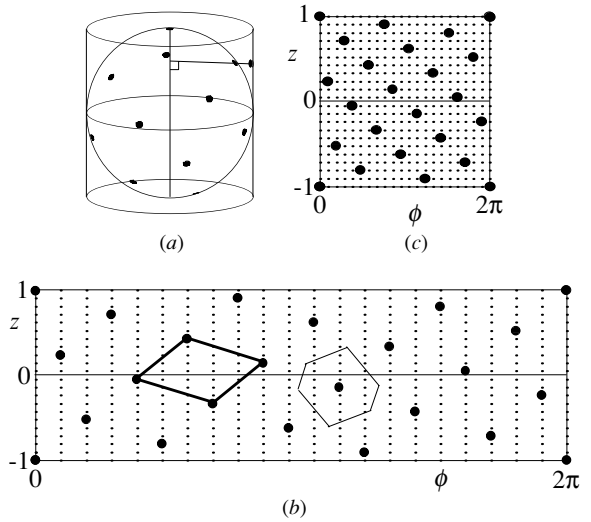

Figure 1. (*a*) The projection between sphere and cylinder. (*b*) The Fibonacci sampling lattice (heavy dots) on the unwrapped cylinder, using $F' = 13, F = 21$ (22 points in total). The points lie on a sublattice of sides $2\pi/21$ and $2/21$. A standard unit cell (heavy) and a Voronoi cell (light) are outlined. (*c*) The picture in (*b*) compressed horizontally to form a square; the lattice is still very evenly spaced.

The standard manoeuvre for elementary numerical integration, which we too adopt, is effectively to puncture the sphere at the top and bottom poles. It is then mapped on to the enclosing vertical cylinder via the Archimedes projection, perpendicularly out from the polar axis (figure 1(*a*)). Since the projection preserves area, integration over the sphere is directly equivalent to integration over the cylinder (the Jacobian is unity). The coordinates $(\phi, \cos\theta)$ on the sphere are thus covered uniformly, as is required. Of course, the value of the projected integrand function will be constant all around each rim of the cylinder, the constants being the pole values. This is associated with the original sphere having no boundary, and it should be possible to integrate this special kind of projected function numerically more accurately than a generic function on a cylinder.

We shall apply two numerical methods in combination. Each individually is advantageous for general cylinder integrations, but the combination is only beneficial for integrand functions derived from a sphere. The first is the use of an oblique lattice of sampling points based on a pair of successive Fibonacci numbers. The idea of using oblique Fibonacci lattices for integrations on flat rectangular domains is fairly well established [5–8]. The rough idea is that if the boundaries are causing the error then there is some advantage in having an integration lattice that is as 'unparallel' to the boundaries as possible, in an arithmetic, number-theoretical sense.

Actually the advantage is rather slight, and further measures to suppress the influence of the boundaries are desirable (for both rectangle and cylinder). We combine Fibonacci, therefore, with a second numerical method: non-uniform scaling, carried over from ordinary one-dimensional numerical integration. This modifies the integrand function in a prescribed manner (independent of the sampling lattice on the cylinder) designed to keep the value of the integral unchanged while making the new integrand function zero on the boundary. Strikingly, in conjunction with Fibonacci, and with appropriate manoeuvring, this scaling method achieves the same order of accuracy, $\sim N^{-6}$, for smooth (C^∞) functions on the sphere

as it achieves for smooth functions in one dimension. This is *in contrast* to rectangles, where non-uniform scaling does improve the accuracy, but only to the order N^{-3}, that it would achieve anyway without Fibonacci. (On p 146 of the useful reference [8], the power is unfortunately misquoted in the text as being bounded above by a faster decay, contradicting the table on the same page, which indeed exhibits the $\sim N^{-3}$ decay.)

2. Constructing the Fibonacci lattice on the cylinder

It is easiest first to describe our basic set of cylinder integration points and refine it later (section 5) for our final prescription. Let the sphere and the cylinder have radius unity. The height of the cylinder, $-1 < z < 1$ ($z = \cos\theta$), is to be divided into a large number F of intervals where F is one of the Fibonacci numbers 1, 1, 2, 3, 5, 8, 13, 21, 34, 55, 89, 144, ... (in this set each number is the sum of the pair before it). We denote the next smaller number in the set by F'. A point is placed at the pole point $z = -1$, and, to start with, F other points are placed at equal intervals $\Delta z = 2/F$ along $\phi = 0$, the whole set being numbered $j = 0$ to F. Each point is now rotated in ϕ by an angle proportional to j, so that its coordinates are $z = -1 + j\Delta z$, $\phi = 2\pi(F'/F)j$. The ratio F'/F is close to the inverse golden ratio, $\frac{1}{2}(\sqrt{5}-1)$. The result (figure 1(*b*)) is a highly sheared lattice in which successive j points are separated by the quite large angle $2\pi(F'/F)$, and in which the most visually prominent unit cell is not based on successive j values. This arrangement is the standard Fibonacci lattice for integration on a rectangle [5–8].

The sampled lattice points on the cylinder lie on an underlying rectangular lattice based on the Fibonacci number F (21 in figure 1(*b*)). The fact that neighbouring Fibonacci numbers share no factors ensures that the vertical period of the lattice on the cylinder is 2 (its height), not less. Around each lattice point one may construct a Voronoi cell (the area of positions closer to this lattice point than any other); one is drawn in the figure. Generically, such cells are six-sided polygons. They are all identical, of course, and are not at all elongated.

A striking property resulting from the strong irrationality of the golden ratio is that any stretching or compression in either axis direction (e.g., figure 1(*c*)) still yields Voronoi cells that are not at all elongated (in fact, for a lattice based exactly on the inverse golden ratio, the cell shape cycles through a one-parameter family). This is in marked contrast to stretching a conventional upright rectangular lattice. We shall refer to our Fibonacci lattice on the cylinder as the 'oblique lattice' and a conventional upright rectangular one, with its equal intervals of ϕ and z (=cos θ on the sphere), as an 'upright lattice'. The shape of the rectangle is arbitrary (but fixed) and will not affect our results.

When the oblique lattice on the cylinder is projected back on to the sphere, it is stretched vertically and compressed horizontally by variable amounts. In consequence, the cells are no longer identical on the sphere but are still nowhere elongated, and the points on the sphere are evenly spaced in all directions (figure 2(*a*)). The array has a familiar appearance of two intersecting spirals; such arrangements are well known in nature, for example, as the pattern formed by the seed heads of a sunflower [9, 10]. This is in contrast with figure 2(*b*) which shows the uneven result of distributing a similar number of points on an upright lattice. The obliqueness means, importantly, that a large number of latitudes are sampled (a different one for each point), reducing the error from the pole coordinate singularities. Although these considerations indicate qualitatively that the oblique lattice may have merit over the upright one, the analysis of the error in the numerical integration (section 4) proceeds in a different way, by Fourier analysis. The specific merit of the Fibonacci ratio is re-examined in section 7.

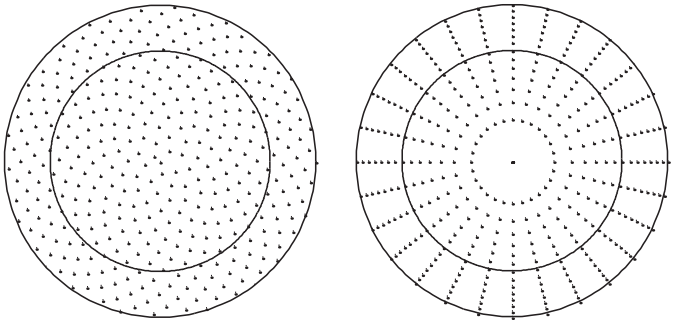

(*a*) (*b*)

Figure 2. Equal area North pole ('Lambert') projection of points on the surface of a sphere. In this projection the point (θ, ϕ) is first moved to $(\frac{1}{2}\theta, \phi)$ on the northern hemisphere, and then projected perpendicularly on to the equatorial plane; equal areas on the surface of the sphere transform into equal areas on the projection; the south pole becomes the whole circumference. The equator is shown. (*a*) Oblique sampling, 378 points using the Fibonacci number $F = 377$. (*b*) Upright sampling, 366 points at equal intervals of $\cos\theta$ and ϕ.

3. Integrand modification by non-uniform scaling

An important attribute of a numerical integration scheme is that it has an error which decreases reasonably fast with the fineness of the sampling lattice. For example, in one-dimensional integration Simpson's rule is superior to the trapezium rule because for smooth integrands it has a faster decay of error with the number of sampling points N ($\sim N^{-4}$, versus $\sim N^{-2}$). An even faster decay is obtained by using the trapezium rule but with a prior non-uniform scaling modifying the integrand function without changing the value of the integral. We shall use such a scaling for our two-dimensional integration on the cylinder, modifying the integrand by scaling the single variable z. This modification is in preparation for numerical integration, but is quite independent of the sampling (upright or oblique, few points or many). The non-uniform scaling we choose, following Sidi [11, 8], is shown in figure 3;

$$z = z' + \frac{\sin(\pi z')}{\pi}, \tag{1}$$

and one then has

$$\int_{-1}^{1} f(z)\,\mathrm{d}z = \int_{-1}^{1} f(z(z'))(\mathrm{d}z/\mathrm{d}z')\,\mathrm{d}z' = \int_{-1}^{1} f'(z')\,\mathrm{d}z' = \int_{-1}^{1} f'(z)\,\mathrm{d}z, \tag{2}$$

defining a new integrand $f' \equiv f \times (\mathrm{d}z/\mathrm{d}z')$. The last equality is a mere renaming of the integration variable so that further reference to z' is avoided.

At the boundaries the new integrand is zero and the lowest non-zero odd derivative is easily found to be the fifth. By the Euler–Maclaurin formula [2] this suppresses the error to a decay $\sim N^{-6}$. As mentioned above, this order of error, $\sim N^{-6}$, will carry over to our sphere integrations (for integrands that are smooth on the sphere). (Lest it be of concern that a smooth function on the sphere, e.g. x, is not a smooth function of z ($x \propto \sqrt{1 - z^2}$), we may state in reassurance that this is dealt with by 'duplication' later ($m = 1$ case). Also relevant (for the $m = 0$ case) is the remark that any smooth function on the sphere, when azimuth-averaged around latitude lines, is a smooth function of z.)

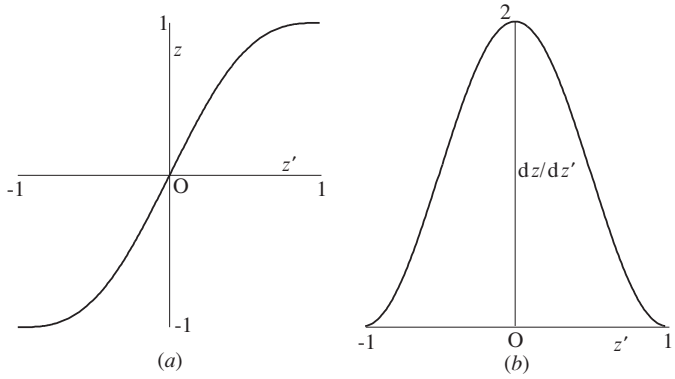

Figure 3. The scaling described by equation (1).

4. Analysis of error in the numerical integral

In practice, to find out how many significant figures in the result of an integration with a given N can be relied on, one integrates again with a higher value of N. (Alternatively, for the sphere one can re-orient the sampling array to judge error.) We shall therefore be content to investigate analytically only the comparative power law decays of errors in our integration scheme and alternatives. (If analytic estimates of coefficients were to be sought they would presumably be found in the dominant Fourier coefficients we identify.) To keep the notation simple we shall refer to the integrand function as f, although in the end we are more interested in the modified integrand function f'. The two cases are distinguished in table 1, to be discussed later.

Our error analysis is to be based on Fourier series on the cylinder. To account correctly for rim sampling it is helpful to imagine both the integrand function and the sampling lattice unwrapped and extended periodically by translation to cover the plane, the periods being 2π and 2. The corresponding top and bottom rim points (one each for the oblique case or more each for upright) will be superimposed and count as one point, not two. In the unperiodized cylinder version, therefore, the rim contributions should be halved, a procedure that amounts to using the trapezium rule for the integration over z. The results of the numerical integration by the upright and oblique lattices can now be compared with the true integral via a Fourier transformation in the following standard way.

The sampling function, $g(\mathbf{r})$ say, is a lattice (upright or oblique) of two-dimensional delta functions in the plane $\mathbf{r} = (\phi, z)$. The delta functions have equal weight $4\pi/N$ where N is the number of sampling points on the cylinder including the point(s) on one rim but not the other. For the oblique lattice $N = F$ and the total number of points on the sphere is $N + 1$. Both $g(\mathbf{r})$ and the periodized integrand function $f(\mathbf{r})$ are represented by Fourier series. Denoting the corresponding spatial frequencies by $\mathbf{K} = (m, \pi n)$, where both m and n are integers ranging from $-\infty$ to ∞,

$$f(\mathbf{r}) = \sum_{m,n} f_{m,n}\, \mathrm{e}^{\mathrm{i}\mathbf{K}\cdot\mathbf{r}}, \qquad g(\mathbf{r}) = \sum_{m,n} g_{m,n}\, \mathrm{e}^{\mathrm{i}\mathbf{K}\cdot\mathbf{r}}, \tag{3}$$

where

$$f_{m,n} = \frac{1}{4\pi} \int_{-1}^{1} \left[\int_{0}^{2\pi} f(\phi, z)\, \mathrm{e}^{-\mathrm{i}m\phi}\, \mathrm{d}\phi \right] \mathrm{e}^{-\mathrm{i}n\pi z}\, \mathrm{d}z, \tag{4}$$

and similarly for $g_{m,n}$.

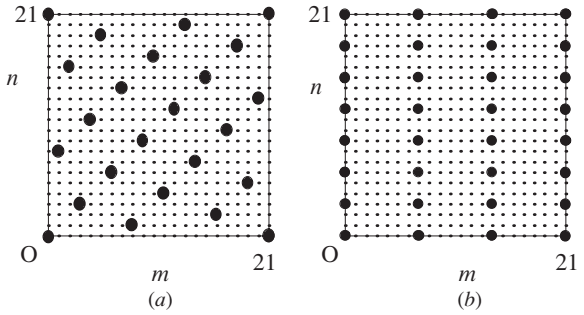

Figure 4. (*a*) The reciprocal lattice (heavy dots) corresponding to the oblique lattice in figure 1(*c*). It is a $\pi/2$ rotated version of the latter. The Fourier transform of the periodized integrand f is a discrete underlying lattice (δ-functions with strengths $f_{m,n}$), indicated by the lighter points. (*b*) The reciprocal lattice (heavy dots) of an upright sampling lattice based on (ϕ, z) coordinates, with exactly the same density of points as the oblique lattice in (*a*).

Thus, m, πn define an underlying lattice in Fourier space $\mathbf{K}$ on which are defined the coefficients $f_{m,n}$ (figures 4(*a*) and (*b*)). These decay in value far from the origin $m = 0$, $n = 0$. On most of the m, πn points the coefficients $g_{m,n}$ are zero; only on the 'reciprocal' lattice [12] of the original sampling lattice $g(\mathbf{r})$ are the Fourier coefficients $g_{m,n}$ unity, rather than zero (heavy dots). By definition, a point (m, πn) is a point of the reciprocal lattice if and only if it obeys the equation, $m\phi + \pi nz = 0 \bmod 2\pi$, for all the sampling points (ϕ, z). It is associated via the equation with a set of equally spaced lines in the real space parallel to lattice lines. The horizontal and vertical periods of the oblique reciprocal lattice (figure 4(*a*)) are $m = F$ and $\pi n = \pi F$ and those of the upright reciprocal lattice are much smaller $\sim\sqrt{N}$ (figure 4(*b*)), depending on the height and width chosen for the rectangular cell.

The convolution theorem [12, 13 section 17.22] may be expressed as

$$\int f(\mathbf{r})g(\mathbf{R}-\mathbf{r})\,\mathrm{d}^2\mathbf{r} = (2\pi)^2 \sum_{m,n} f_{m,n}g_{m,n}\,\mathrm{e}^{\mathrm{i}\mathbf{K}\cdot\mathbf{R}}, \tag{5}$$

where the integration is over the cylinder ($2\pi \times 2$). Taking $\mathbf{R} = 0$ and noting that $g(\mathbf{r})$ is centrosymmetric, we have for the numerical integral

$$\int f(\mathbf{r})g(\mathbf{r})\,\mathrm{d}^2\mathbf{r} = (2\pi)^2 \sum_{m,n} f_{m,n}g_{m,n}. \tag{6}$$

This expresses the numerical integral as (proportional to) the sum of the products of the pairs of coefficients on *all* the jointly occupied lattice points over the whole plane.

If, in equation (6), we temporarily take $g(\mathbf{r}) \equiv 1$, instead of a lattice of delta functions, the left-hand side is the value of the exact integral over the unit sphere. All the coefficients $g_{m,n}$ are then zero except for $g_{0,0}$, which is unity, and it follows that the exact integral is $(2\pi)^2$ times the product $f_{0,0}g_{0,0}$. So we reach the well-known result [7, 8] that the error (the difference between the numerical and exact integrals) is $(2\pi)^2$ times the sum of all off-origin coefficient products. It is this, therefore, that must be made as small as possible by choice of the sampling lattice $g(\mathbf{r})$. We shall find that when the number of sampling points is large the off-origin sum is dominated by particular Fourier coefficients.

The Fourier coefficients of the integrand function $f_{m,n}$ decay rapidly away from the origin in the horizontal direction (i.e., with increasing $|m|$), faster than a power law provided the function is analytic [3]. In the vertical direction (i.e., with increasing $|n|$), the decay obeys a power law, but a *different* power law for different vertical columns of points, as follows. The

Table 1. Asymptotic decay rates of Fourier coefficients of the integrand f are shown in the top row, and of the non-uniformly scaled integrand f' in the next row. Finally, in the third row a combination of values of $m = 0$ coefficients associated with the trapezium rule is given. Only for the $m = 0$ column do our lattices use the combinations; the upright has only $m = 0$ entries, and the oblique one has $\pm n$ symmetry only in this column (see, e.g., figure 4(*a*)).

	$m = 0$	$m = 1$	$m = 2$
$f_{m,n}$	n^{-1}	$n^{-3/2}$	n^{-2}
$f'_{m,n}$	n^{-3}	$n^{-9/2}$	n^{-6}
$f'_{m,n} + f'_{m,-n}$	n^{-6}	Not used	Not used

entries in the mth column away from the one through the origin have azimuthal dependence $e^{im\phi}$ and hence derive from spherical harmonics of f with this same azimuthal dependence. (A given harmonic is associated with all points in its column, not just one.) The far-away decay of $f_{m,n}$ vertically is governed by the power law behaviour of the spherical harmonics near the poles in the real space. This is because periodization of the cylinder by translation produces discontinuities in the integrand function and its derivatives at the rims (poles). The local form is $\delta z^{|m|/2}$ [13, formula 8.812], where $\delta z = 1 - \cos\theta$ at the top rim ($\theta = 0$) or $\delta z = 1 + \cos\theta$ at the bottom rim ($\theta = \pi$). It is these discontinuities that in turn govern the magnitudes of the high Fourier coefficients. For large n,

$$f_{m,n} \sim \left| \int \delta z^{|m|/2} \, e^{-in\pi z} \, dz \right| = n^{-|m|/2-1} \times \text{integral independent of } n \qquad (7)$$

(by changing the variable to nz). The slowest decay determines the error. For the upright lattice which has no low $|m|$ entries except on $m = 0$ (figure 4(*b*)), the n-values of the reciprocal lattice points along this $m = 0$ axis have the slowest decay and are multiples of $\sim\sqrt{N}$. For the oblique reciprocal lattice the n-values on the $m = 0$ axis are multiples of N, but there are also entries in the columns $|m| = 1, 2, \ldots$ with n-values again of order N. The fact that there are (infinitely) many entries in each column does not affect the power law dependence of error, but only the coefficient, which does not concern us.

For the Fourier coefficients of the modified function integrand f' arising from the prior non-uniform scaling (1), the equivalent results are obtained by recognizing that $\delta z \sim \delta z'^3$ near the rims, so that m is replaced by $3m$. Also, though, there is an extra factor $\sim\delta z'^2$ from the Jacobian dz/dz', so $f'_{m,n} \sim n^{-|3m|/2-3}$.

The top row of table 1 shows the asymptotic n dependences of $f_{m,n}$ for $m = 0$ to 2, from equation (7), and the next row the equivalent results for $f'_{m,n}$. Evidently, the latter are decaying faster and we concentrate on this non-uniformly scaled case from now on. The $m = 0$ entry n^{-3} has the slowest decay. However, this dependence is replaced by the decay n^{-6} shown in the third row of the table if one combines the coefficients on the two sample points $(0, \pm n)$ (for both upright and oblique sampling lattices we shall be summing all sampled contributions). The reason for the cancellation of the n^{-3} decay is that it arises from the discontinuities at the cylinder rims and the discontinuities have an antisymmetrical Fourier transform. The cancellation is implicit in ordinary (trapezium rule) integration, which has order of error n^{-2} for the unmodified case and n^{-6} for the modified case.

For the columns near the $m = 0$ one there are no lattice points of the upright Fourier lattice, so *only* the $m = 0$ column is relevant and the dominant term is n^{-6} for f', which with $n \sim \sqrt{N}$ as the vertical period of the upright lattice gives an error $\sim N^{-3}$. The oblique Fourier lattice does have lattice points near the $m = 0$ axis, with the slowest decay coming from $m = 1$, giving a decay $n^{-9/2}$ for f'. Such off axis ($m \neq 0$) coefficients are not partnered

with cancelling ones, since both m, $\pm n$ are not sampled, so they remain undiminished by the trapezium rule decay. Since by design $N \sim n$ for the oblique lattice, the decay is $N^{-9/2}$. However, this dominant $N^{-9/2}$ decay can be removed by a straightforward manoeuvre (next section), improving the accuracy to the next most dominant power N^{-6}.

5. Error reduction by duplication, and final result

There is a straightforward method for reducing the error of the oblique Fibonacci lattice by eliminating the dominant $N^{-9/2}$. The real space Fibonacci lattice, the periodized cylinder lattice, is simply shrunk horizontally by a factor 2; the consequence for the Fourier, reciprocal, lattice is that it stretches horizontally by a factor 2. This means that all odd-numbered columns m are vacated; in particular the $n^{-9/2}$ from $m = 1$ is eliminated, and the power n^{-6} is now dominant. On the sphere the shrink corresponds to halving the twist angle between successive latitude circles to $\pi F'/F$ and then reproducing the arrangement by rotation of π about the polar axis, 'duplication'.

Explicitly our Fibonacci numerical integration formula for the sphere is

$$\int_{-1}^{1}\int_{0}^{2\pi} f(\phi, z)\,\mathrm{d}\phi\,\mathrm{d}z \approx \pi\ \Delta z \sum_{j=0}^{F}[1+\cos(\pi z_j)]\left\{ f\left(\frac{\pi j F'}{F}, z_j + \frac{\sin(\pi z_j)}{\pi}\right) + f\left(\pi + \frac{\pi j F'}{F}, z_j + \frac{\sin(\pi z_j)}{\pi}\right)\right\} \tag{8}$$

where $\Delta z = 2/F$, $z_j = -1 + j\ \Delta z$, and F' and F are successive Fibonacci numbers.

6. Numerical verification

As well as choosing a particular integrand function to verify the error decay powers derived above, we shall proceed more generally and analytically as far as possible. We consider a random ensemble of integrand functions specified by independent random coefficients of spherical harmonics Y_J^m. The scale size or wavelength of the undulations is determined by the J values for which the coefficients are large (mean square), and there is no essential loss of generality in choosing just a single J value to have non-zero coefficients a_m, identically distributed. The motivation for this procedure is that the mean square error can be evaluated *analytically*, although the result requires numerical tabulation. For any $J > 0$, the true integral for any member of the ensemble is zero (since spherical harmonics are orthogonal to the constant one, Y_0^0), so the error is simply the sum of the values at the sampling points times $4\pi/N$. The mean square error is therefore (with $\langle a_m a_M^* = \delta_{mM}\rangle$) given by

$$\langle \mathrm{Error}^2\rangle/(4\pi/N)^2 = \left\langle \sum_{\substack{\text{Sampling}\\ \text{points}_i}} \sum_{m=-J}^{J} a_m Y_J^m(\phi_i, z_i) \sum_{\substack{\text{Sampling}\\ \text{points}_j}} \sum_{M=-J}^{J} a_M^* Y_J^{M^*}(\phi_j, z_j)\right\rangle \tag{9}$$

$$= \sum_{\substack{\text{Sampling}\\ \text{points}_i}} \sum_{\substack{\text{Sampling}\\ \text{points}_j}} \sum_{m=-J}^{J} Y_J^m(\phi_i, z_i) Y_J^{m^*}(\phi_j, z_j) \tag{10}$$

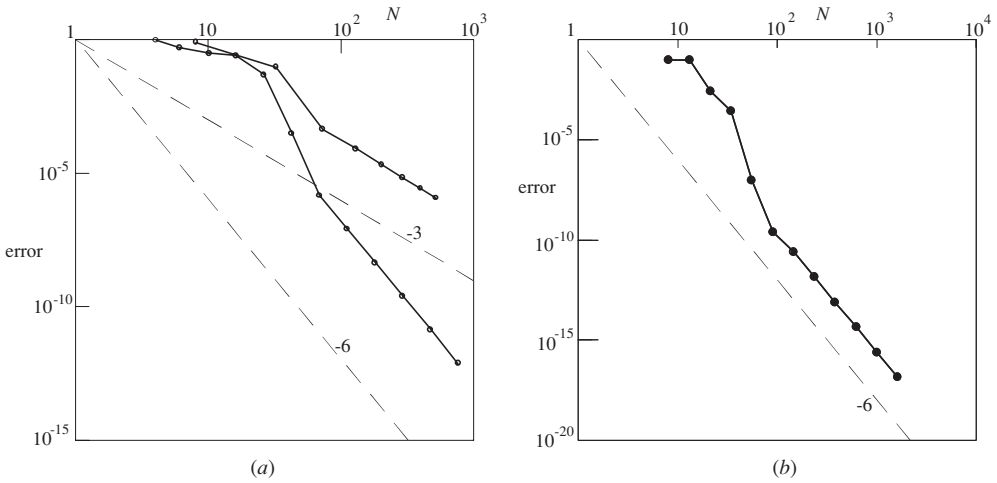

Figure 5. Log–log plots of error versus total number of points, N. The numbers indicate the slopes (the power laws). (a) Result of the double summation in equation (12) with $J = 4$: oblique sampling (Fibonacci) (with non-uniform scaling and duplication of points) (slope -6); upright sampling (with non-uniform scaling) (slope -3). (b) Integration of $f = x^2y^2\,\mathrm{e}^z$ (rotated), using oblique sampling (Fibonacci) (with non-uniform scaling and duplication of points) and with ordinary (trapezium rule) integration for z (slope -6). For both (a) and (b) there is an unexpected steep drop before the asymptotic form is reached (for $N \gg J^2$ in (a)).

$$= \left(\frac{2J+1}{4\pi}\right) \sum_{\substack{\text{Sampling}\\ \text{points}\,i}} \sum_{\substack{\text{Sampling}\\ \text{points}\,j}} P_J\left(z_i z_j + \sqrt{1-z_i^2}\sqrt{1-z_j^2}\cos(\phi_i - \phi_j)\right) \tag{11}$$

$$= \left(\frac{2J+1}{4\pi}\right) \sum_{\substack{\text{Sampling}\\ \text{points}\,i}} \sum_{\substack{\text{Sampling}\\ \text{points}\,j}} P_J(\hat{\mathbf{i}}\cdot\hat{\mathbf{j}}) \tag{12}$$

where the argument $\hat{\mathbf{i}} \cdot \hat{\mathbf{j}}$ of the Legendre polynomial is the cosine of the angle between the directions of the sampling points i and j [13, formula 8.794]. This double summation over the sampling array requires numerical evaluation. Of course, the larger the J value chosen, the greater will be the number of sampling points required to reach the asymptotic regime, so a small value ($J = 4$) will suffice. The lines in figure 5(a) are seen to have the predicted slopes when N becomes sufficiently large.

Figure 5(b) shows the error computed for a particular choice of integrand function whose integral is known exactly. To avoid symmetry the integrand was taken to be the function $f = x^2y^2\,\mathrm{e}^z$, rotated by an arbitrary amount (in fact specified by Euler angles 0.9, 0.3, 0.3). The slope on the log–log plot becomes -6, as expected.

7. Further discussion

We conclude with remarks on three matters arising from our description.

(1) A Fibonacci ratio in the lattice construction (section 2) is preferred, rather than any other ratio, because of the strong irrationality of the (inverse) golden ratio $\frac{1}{2}(\sqrt{5}-1)$

of which it is a continued fraction approximant—a truncation of $1/(1+1/(1+\cdots))$. This ensures an oblique sampling lattice in which the associated reciprocal lattice points (Fourier sampling points) are 'kept away' as well as possible, in the following sense, from the columns closest to $m=0$ which are mainly responsible for the error. For this description we may consider the basic lattice, prior to the two-fold horizontal scaling, so the columns in question are $m=\pm 1$. Consider the oblique lattice based, not on Fibonacci numbers F', F, but on any pair of positive integers (with no common factors) P', P. It is simplest to speak of both original and reciprocal lattices as scaled so as to lie on the integers; thus the original lattice comprises all the points which are multiples of the vector $(P', 1)$ mod P. This lattice has a reciprocal lattice: all integer vectors p', p which satisfy $p'P' + p \times 1 = 0 \bmod P$. (This turns out to be just a $\pi/2$ rotated copy of the original lattice.) The minimum value of the product $|p'p|$ for any reciprocal lattice point off the axes is proven [7] to lie between the bounds $P/(a+2) \leqslant |p'p| \leqslant P/a$, where a is the largest continued fraction element of the fraction P'/P. Thus, $|p'p|$ is of order P and a should be as small as possible. Evidently, Fibonacci pairs $P' = F'$, $P = F$, alone, have $a = 1$ and therefore the largest lower bound on $|p'p|$. For Fibonacci pairs the minimum product $|p'p|$ is equal to F'' [7] (coming from $p' = \pm 1$, $p = F''$), where F'' is the Fibonacci number preceding F'.

(2) For experimental measurements over the surface of a sphere the interpretation of formula (8) is perhaps somewhat surprising, and merits comment. We have deliberately interpreted the non-uniform scaling as being applied to the integrand, maintaining the sampling array unchanged. Operationally, however, (8) dictates that the original integrand function should be sampled at an array of points unevenly spaced in z (namely the values $z_j + \sin(\pi z_j)/\pi$ in (8)), thus over-sampling near the poles but with a corresponding down-weighted contribution from $\mathrm{d}z/\mathrm{d}z'$. So even sampling is *not* optimal. The lesson is once again that the 'puncturing' of the sphere, implicit in the projection from the cylinder, is asymptotically the source of error in the numerical integration. Uneven spacing (while still locally reasonably isotropic) around each point is needed to compensate for the distinguished axis. An alternative scheme, which preserves the even sampling but which is not so effective as the non-uniform scaling we have described, would be to use Simpson's rule, that is weight points $\frac{1}{3}, \frac{4}{3}, \frac{2}{3}, \frac{4}{3}, \frac{2}{3}, \ldots, \frac{4}{3}, \frac{1}{3}$ from pole to pole (F even is required) and not to use duplication but six-fold replication together with twist $\pi F'/3F$ between latitudes. Simpson helps compensate for the distinguished axis, giving $\sim N^{-4}$ accuracy.

(3) Mention should be made of an entirely different, non-elementary, method of numerical integration on a sphere based on a conventional method in one dimension. 'Gaussian quadrature' for integration on a one-dimensional interval $-1 < z < 1$ uses J unequally spaced points with unequal weightings based on Legendre polynomials [2, section 4.5], and achieves the exact result when integrating any polynomial up to order $2J-1$. This can be adapted straightforwardly to a sphere using $2J^2$ points by placing J points, at the specified values of z, along each of $2J$ equally spaced semicircles of longitude. These semicircles ensure that any function with ϕ variation $\exp(\mathrm{i}m\phi)$ and $0 < |m| < J$ correctly integrates to zero for each z. The Gaussian quadrature in z then exactly integrates the $m=0$ spherical harmonics (Legendre polynomials in z) up to order $2J-1$. Thus, any spherical harmonic up to order $2J-1$ has been integrated exactly. Other non-elementary schemes for numerical integration on the sphere are under development [14].

Acknowledgments

We should like to thank the referees for their useful suggestions for improvements.

References

[1] Nye J F 2003 A simple method of spherical near-field scanning to measure the far fields of antennas or passive scatterers *IEEE Trans. Antennas Propagation* **51** 2091–8

[2] Press W H, Flannery B P, Teukolsky S A and Vetterling W T 1992 *Numerical Recipes* (Cambridge: Cambridge University Press)

[3] Arnold V I 1983 *Geometrical Methods in the Theory of Ordinary Differential Equations* (Berlin: Springer)

[4] Neutsch W N 1996 *Coordinates* (Berlin: Walter de Gruyter) pp 964–5

[5] Zaremba S K 1966 *Ann. Mat. Pure Appl.* **73** 293–317

[6] Niederreiter H and Sloan I H 1994 Integration of non-periodic functions of two variables by Fibonacci lattice rules *J. Comp. Appl. Math.* **51** 57–70

[7] Niederreiter H 1992 *Random Number Generation and Quasi-Monte Carlo Methods* (Philadelphia, PA: SIAM)

[8] Sloan I H and Joe S 1994 *Lattice Methods for Multiple Integration* (Oxford: Oxford University Press)

[9] Conway J H and Guy R K 1996 *The Book of Numbers* (Berlin: Springer)

[10] Stewart I 1997 *The Magical Maze* (London: Wiedenfeld and Nicolson) p 30

[11] Sidi A 1993 A new variable transformation for numerical integration *Numerical Integration IV, International series of Numerical Mathematics* vol 112 ed H Brass and G Hammerlin (Basel: Birkhausser) pp 359–73

[12] Lipson S G, Lipson H and Tannhauser D S 1995 *Optical Physics* 3rd edn (Cambridge: Cambridge University Press) chapter 4.6

[13] Gradshteyn I S and Ryzhik I M 1980 *Table of Integrals, Series, and Products* (translated by A Jeffrey) (New York: Academic)

[14] Sloan I H and Womersley R S 2004 Extremal systems of points and numerical integration on the sphere *Adv. Comput.* at press